A MOLECULAR DYNAMICS STUDY OF EFFECT OF POLYETHYLENE OXIDE ARCHITECTURE ON SELF-ASSEMBLY OF CARBON NANOTUBES

by

Pushyami Atluri

A thesis submitted to the faculty of
The University of Utah
in partial fulfillment of the requirements for the degree of

Master of Science

Department of Materials Science and Engineering

The University of Utah

August 2011

The University of Utah Graduate School

STATEMENT OF THESIS APPROVAL

The thesis of **Pushyami Atluri**

has been approved by the following supervisory committee members:

Grant D. Smith	, Chair	**date approved** (Date Approved)
Dmitro Bedrov	, Member	**date approved** (Date Approved)
Ashutosh Tiwari	, Member	**date approved** (Date Approved)

and by **Anil V. Virkar**, Chair of the Department of **Materials Science Engineering**

and by Charles A. Wight, Dean of The Graduate School.

ABSTRACT

Carbon nanotubes aggregate strongly to form bundles. One of the ways to control their dispersion is by grafting polymers onto the carbon nanotubes surface. Coarse grained implicit solvent Molecular Dynamics (MD) simulations were used to study the influence of poly (ethylene oxide) (PEO) grafted onto the walls of two single walled carbon nanotubes in water. The system was investigated utilizing both real and repulsive potentials.

The chain length and grafting density of PEO were varied to study their effect on aggregation of carbon nanotubes. PEO has an attractive interaction with the carbon nanotubes which causes aggregation, but at very close distances introduces a repulsive barrier which prevents the nanotubes from aggregating. These competing effects are incorporated into the free energy of the system. It was found that the free energy of the system can be manipulated by changing the chain length and grafting density of the PEO. Simulations investigated the importance of individual contribution of nanotube-PEO and PEO-PEO interaction in water, as well as importance of these contributions to the total energy with respect to changing molecular weight of PEO.

TABLE OF CONTENTS

LIST OF FIGURES

ACKNOWLEDGEMENTS

I would like to thank my research advisor Dr. Grant Smith for his patience and express my deep appreciation to Dr. Dmitry Bedrov and Dr. Justin Hooper for their continuous support and help. This work was funded by MRSEC.

CHAPTER 1

INTRODUCTION

Application of carbon nanotubes is limited by their dispersion in common organic solvents and modification of carbon nanotube surface with polymers is one of the widely researched routes to control their dispersion (1). Molecular dynamics simulations are used to study carbon nanotubes tethered with PEO. The first chapter discusses the various structures and properties of carbon nanotubes. The following chapter discusses why PEO is used in our simulations. In the final chapter, the carbon nanotube-PEO system as a whole is discussed along with the importance of work done.

1.1 Carbon nanotubes

Carbon nanotubes (CNT) are one-dimensional carbon nanoparticles, considered to be curved graphitic structures, with remarkable electrical and mechanical properties owing to their dimensionality (2). The carbon atoms in CNT are similar to those found in graphite, connected by strong covalent bond (sp^2 hybridization) where each carbon atom is bound to three other atoms. Their structures can be mainly categorized as single walled carbon nanotubes (SWCNT) and multi walled carbon nanotubes (MWCNT). They can also be categorized by the way a graphene sheet is rolled up.

SWCNTs are structurally similar to a single layer of graphite wrapped into a tube. MWCNT consist of multiple rolled concentric layers of graphene sheets or concentric cylinders of SWCNT with distance between the two tubes being equal to that of distance between layers in graphite.

There are three ways in which graphene can be rolled into a sheet: armchair, zigzag and chiral. The way a graphene sheet is rolled is represented by a chiral vector denoted by (*n,m*) (3) . The arm chair configuration has *n*=*m* designation and has metallic properties. The zigzag configuration is characterized by *m*=0 and is semiconducting. Lastly the chiral configuration has other values of *n* and *m* and is semiconducting.

CNTs are prepared by three main routes: carbon arc discharge, laser ablation and chemical vapor deposition (4,5,6). CNTs are very strong and stiff due to the strong sp^2 carbon-carbon bond. They can be metallic or semiconductors depending on their chirality as described above. CNTs are good thermal conductors along the tube but insulators perpendicular to tube axis (7). CNTs have promising uses in biomedical, composite materials and electronics applications. Potential applications of CNTs include conductive and high-strength composites, energy storage and conversion devices, sensors, field emission displays and radiation sources, hydrogen storage media, nanometer sized semiconductor devices, probes, and interconnects (8,9).

SWCNTs have strong interactions and aggregate to form bundles or ropes due to strong Van Der Waals forces. This aggregation has been found to act as an obstacle for most applications and results in reduced mechanical and electrical properties as compared to theoretical predictions. SWCNTs pack into ropes of 100-500 tubes and pack in a triangular lattice (10). Hence it has been difficult to achieve their uniform dispersion.

Many methods have been since devised to disperse individual CNTs (1). There are two main routes for the modification of CNT surface. First one is covalent attachment of functional groups to the wall of the nanotube and second is non covalent attachment. Covalent and ionic modifications alter the structural, mechanical and electrical properties of the tubes by introducing defects and internal stresses into CNT. Covalent attachment of polymers to nanotubes improves the efficiency of load transfer in a matrix. While in non covalent methods, there are weak forces between the nanotube surface and polymer that lead to poor load transfer. The physical properties of the nanotube, however, remain unchanged by this method.

CNTs have strong direct nanoparticle-nanoparticle interaction; this interaction dominates and drives the association in water. It has been reported that the water induces repulsive interactions between CNTs similar to what was found in fullerenes (11). There are strong dispersion interactions between water and carbon nanoparticles. These dispersion interactions increase with decreasing nanoparticle curvature, as the curvature decreases there is higher density of carbon atoms on the surface of the particles. Carbon nanotubes have a strong tendency to aggregate. This tendency of aggregation reduces in water when compared to vacuum. Carbon nanotubes will aggregate not because of hydrophobic interactions with water but because of the strong Van Der Waals forces present between the tubes. The water reduces the tendency of aggregation as compared to vacuum. In the simulations carried out, this effect of interaction of water with SWCNT is implicitly included in the potentials, which are described further in the methods section.

1.2 Poly ethylene oxide

Poly ethylene oxide (PEO) is a polymer having structure (-CH_2-O-CH_2-)n. PEO has useful properties such as a wide range of solubilities, lack of toxicity and immunogenicity, nonbiodegradability, and is thus used extensively as a covalent modifier of a variety of substrates (12). PEO is a biocompatible material and has been used widely in bioengineering applications like drug delivery, modification of surface for biocompatibility, tissue engineering, etc. (13,14).

PEO has been used previously to modify the surface of C60 fullerenes to control their dispersion in aqueous solutions (15). PEO has been studied to achieve controllable clusters of C60. This study extends the previous studies on C60 to CNT. CNT is similar to C60 chemically, both have sp^2 hybridized orbitals. Dispersion of CNT will be different than C60 due to effects of curvature arising from high dimensionality of CNT; therefore the results from CNT will be significantly different from C60.

1.3 Scope of current work

Due to aggregation of tubes, their properties are reduced as discussed in section 1.1. Uniform dispersion of tubes opens up wide avenues for applications tapping their unique properties. For example, polymer nanocomposites have enhanced electronic, thermal and optical properties. The forces between the particles depend on the molecular weight of the polymer and their interaction with the aqueous solution. By modifying the surface of the tubes through attachment of polymer, in principle the interaction between the tubes can be controlled by creating a repulsive barrier. Previous MD simulations on fullerenes whose surface has been modified by grafting PEO have shown that fullerenes

don't phase separate but form clusters. The shape and size distribution of these clusters could be controlled by modifying the molecular weight and architecture of grafted PEO (15). In this paper MD simulations are used to investigate the self-assembly behavior of surface modified nanotubes in aqueous solution.

PEO chains have an attractive interaction with SWCNT in water. Even though PEO is soluble in water there is a slight attraction between PEO chains in water. Due to these different interactions it is expected that PEO would reduce the tendency of SWCNTs to phase separate in water. In this paper two SWNTs grafted with PEO chains separated by a distance are investigated, as shown in Figure 1.1. When the two tubes are sufficiently far apart there is no effect of PEO chains from the other SWCNT. As the SWCNT's are brought closer, PEO chains from one tube start interacting with each other and with the other tube. As the distance between the tubes is further reduced PEO chains give rise to entropic effects. This interplay between the energetic and entropic effects gives rise to complex behavior. The depth and distance of attraction and the repulsive barrier can be controlled by changing the architecture, that is, chain length and grafting density of PEO chains.

Previous simulation studies on PEO and SWCNT have reported presence of a purely repulsive barrier as the tubes are brought closer together (16). Experimentally CNTs have been dispersed uniformly by grafting PEO-PPO block copolymers (17). Grafting PEO or any polymer on CNT is one of the ways to control their aggregation as discussed in section 1.1, other simulation studies have explored using block copolymers

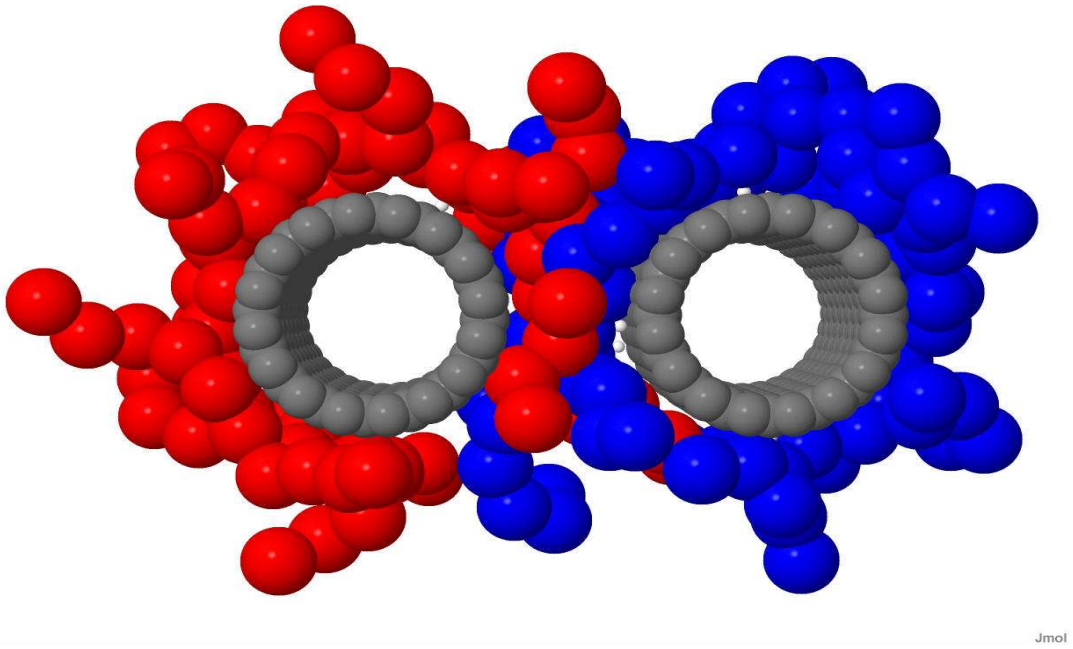

Figure 1.1 : Two SWCNTs separated by a distance of 6A between their surfaces. Red and blue color beads represent PEO tethered onto the surface of two SWCNT.

for the same purpose. Simulations and experiments have also been carried out for CNT in a matrix of polymers where the polymers wrap around the CNT and form an interface (18,19,20).

This work primarily targets at understanding the aggregation behavior when the tubes are anchored with PEO. This work also aims to understand how the behavior of the systems change by changing the architecture of PEO. Finally this study also aims to understand which are the important factors that drive the phase behavior of the system.

The set up of the simulations and the parameters are described in the methods section. The potentials that describe the interaction between PEO with water, CNT with water and PEO grafted CNT in water are described in the potentials section of Methods chapter. The results chapter is divided into three main sections. The first section discusses the brush profiles for different architectures and molecular weights of PEO. The second section discusses the free energy of systems from which we can deduce the behavior of the system as the two SWCNTs grafted with PEO are brought close together. The second section also discusses the contribution of thermodynamic parameters (energy and entropy) to the free energy of the system. The last section investigates the individual contributions of different interactions between SWCNT and PEO.

CHAPTER 2

METHODOLOGY

2.1 Simulation details

Two SWCNTs are placed parallel to each other. The SWCNTs used in our simulations have chirality (16,0) which is a zigzag configuration. The diameter *d* of the SWCNT can be calculated using

$$d = \frac{a}{\pi}\sqrt{n^2+nm+m^2}$$

where a = 2.461 A ; n=16 ; m=0. Each of the SWCNTs has PEO grafted on them which varies in chain length and grafting density in the 13 systems that we simulate. The chain lengths vary as 3, 6, 12 and 24 monomers per chain and the grafting densities vary as 8, 16, 32 PEO chains per tube. All the thirteen different systems are shown in Table 2.1. Table 2.1 shows number of PEO monomers/beads per unit area of the SWCNT for each of the system. The area of SWCNT in the simulations is $1506.27A^2$

We use the notation X_PEO_Y where X is the grafting density of PEO chains per SWCNT and Y is the chain length per graft.

Table 2.1 :Different simulated systems varying in PEO architecture.

Number of PEO monomers per unit area of SWCNT(A^2)

Grafting density Chain length	8 chains/ SWCNT	16 chains/SWCNT	32 chains/SWCNT
3 chains/graft	0.016	0.032	0.064
6 chains/graft	0.032	0.064	0.127
12 chains/graft	0.064	0.127	0.255
24 chains/graft	0.127	0.255	0.510
36 chains/graft	0.191	----	----

PEO is attached to the tube through grafting points on the surface of SWCNT. The tubes grafted with PEO are initially separated by a large distance. This furthest distance of separation is the distance at which it is expected that, there will be no interaction between PEO chains on one tube with PEO chains on the second tube. For short chain systems the furthest distance between surface of two tubes is smaller than for longer chain systems. For example, for the 8PEO6 system the furthest distance between tubes is 40A whereas for 8PEO24 system the tubes are separated by 80A. As simulation proceeds, the two tubes that are constrained parallel to each other are brought closer together from their distance of farthest separation. The tubes are brought closer together in steps of 1A. Therefore, if the furthest distance between surface of tubes is 40A, it takes 40 steps to bring the two tubes close such that their surfaces are touching. Initially, at each step all the systems were sufficiently equilibrated to allow the PEO chains to attain the lowest energy conformation. Once each of the thirteen systems were sufficiently equilibrated

they were run for longer times. We simulate the systems for 50 ns at each separation.

Figure 1.1 shows system 8PEO12, which is each SWCNT having 8 grafted chains each having chain length of 12 PEO monomers. The distance between surface of tubes is 6A. The figure clearly shows PEO originating from different tubes in different colors. It can be seen that PEO from one tube is interacting with PEO of other tube at this close distance. Figure 2.1 shows the same 8PEO12 system but the tubes are separated by 39A and it can be seen that the PEO from two tubes do no interact. For better statistics all the systems were run with different initial configurations.

Simulations in this study are carried out at room temperature (298K). At this temperature PEO of any molecular weight or concentration is soluble in water. The ether oxygen of PEO forms hydrogen bonds with water molecules. The CH_2 group in PEO is hydrophobic. At higher temperature the solubility of PEO in water decreases due to a decrease in hydrogen bonding and an increase in hydrophobic interaction between the PEO chains. The amphiphilic nature of PEO is captured in the coarse grained model which is used. The PEO chains are such that they do not wrap around the SWCNT it originates from (to the tube it is anchored), due to presence of stiffness in the chain.

In the simulations carried out in this study, it doesn't matter which method (covalent and non covalent methods, discussed in section 1.1) has been adopted to attach the polymer to the surface. The system is set up such that the PEO is anchored to an adsorbing molecule which are called as dummy atoms. These adsorbing molecules (dummy atoms) give sufficient physical adsorption to keep the chain adsorbed to the surface. As the main aim of the study is to examine how the surface modification affects aggregation, the details of which chemical process these simulations are equivalent to is

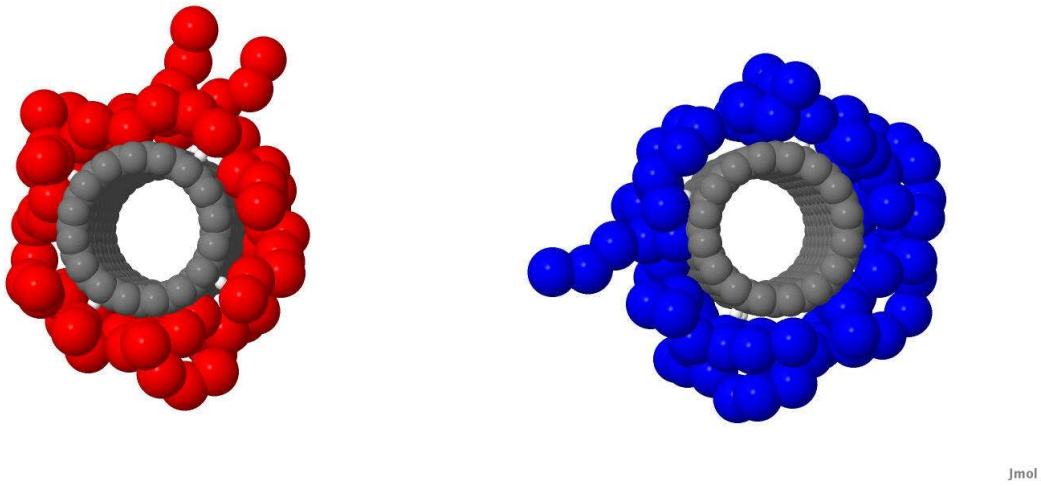

Figure 2.1: Two SWCNTs separated by a distance of 39A between their surfaces. Red and blue color beads represent PEO tethered onto the surface of two SWCNT.

not discussed.

All simulations were carried out using LUCRETIUS (21) which is a freely available simulation package. Brownian integrator was used and simulations were carried out at room temperature (298 K) in constant volume (NVT) ensemble. Periodic boundary conditions were implemented only in the Z direction which implies that the tube has an infinite length.

2.2 Potentials used

There are three different types of interactions in the system, tube-tube interaction, tube-PEO interaction and PEO-PEO interaction. The tube-tube interaction is described by Van Der Waals interaction. It remains the same irrespective of the PEO architecture, hence this interaction is not added when the results are reported. This interaction between the two SWCNTs in our system is shown in Figure 2.2 for reference. The two SWCNTs have a strong attraction and a deep well at center to center separation of around 15.9 A. It is due to this deep well of attraction that the tubes have a strong tendency to aggregate and form bundles. To prevent the tubes from aggregating the tubes should not be allowed to reach the separations at which the deep minima occurs. The r=0 is the position of center of mass of SWCNT. The tube-PEO and PEO-PEO interactions are described by a numerical potentials which has the form of a Lennard Jones (LJ) (22) potential. We refer to this potential as the full potential or the real potential.

The real interaction/full potential between tube-PEO and PEO-PEO are shown in Figure 2.3.

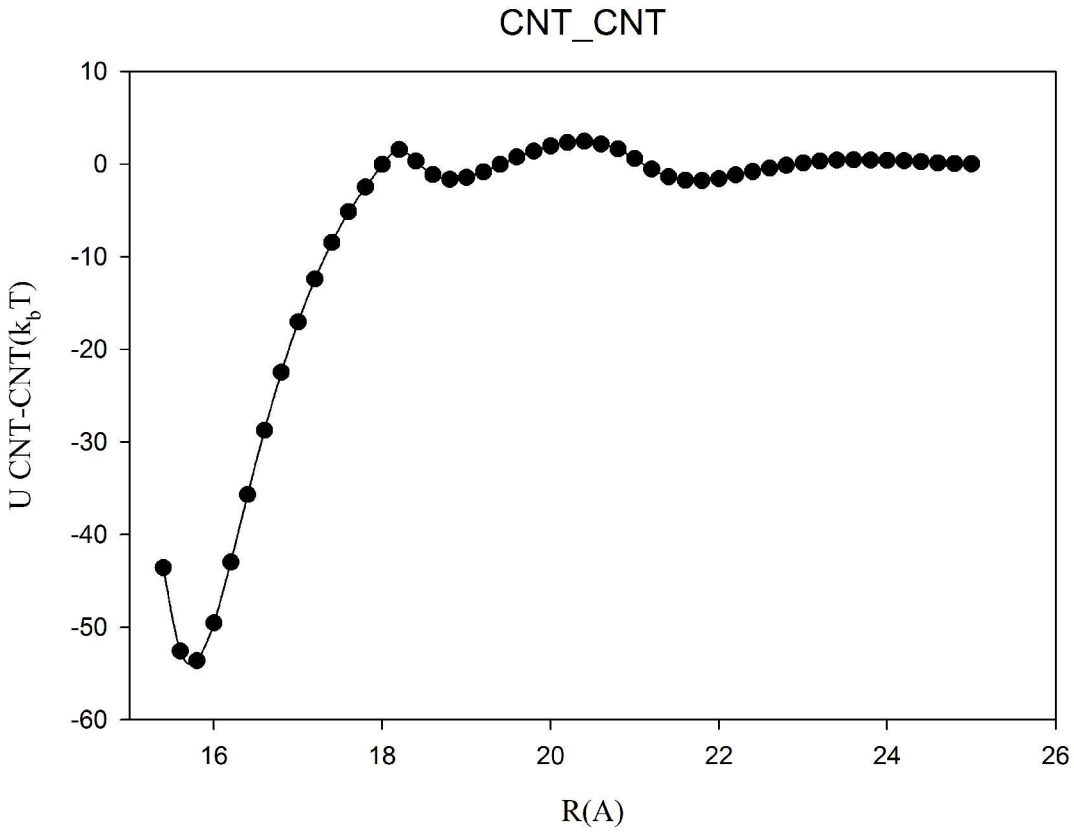

Figure 2.2: Interaction between two bare SWCNT in water.

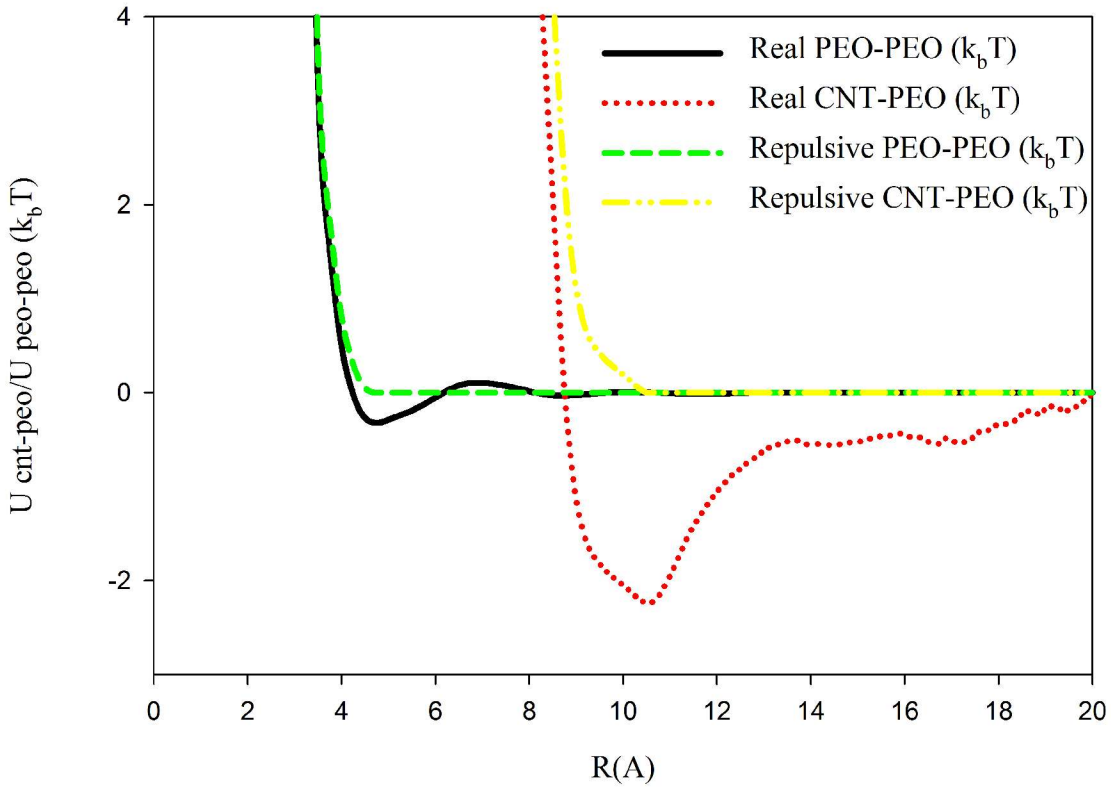

Figure 2.3: Different interaction potentials between tube-PEO and PEO-PEO.

Simulations are also carried out using repulsive numerical potentials that have the form of Weeks Chandler Anderson (WCA) potentials (23). The repulsive potentials are obtained from truncation of the real potentials. It has the same shape as real potential unto the minimum in the curve but does not include the attractive dispersion tail of real potentials. The green line represents the repulsive potential between PEO-PEO and the black line shows the repulsive potential between CNT-PEO. There are two main interactions in the system, that is, between tube-PEO, PEO-PEO. Each interaction is described by both real and repulsive potentials. Therefore, there are different combinations possible to define the total interactions in the system. The four combinations are, interaction between tube-PEO and PEO-PEO is attractive (Real); interaction between tube-PEO is repulsive but PEO-PEO is still attractive (Repulsive_CNT PEO); tube-PEO is attractive but PEO-PEO is repulsive (Repulsive_PEO PEO); when both tube-PEO and PEO-PEO are repulsive (Repulsive_All). All the pairs of potentials that we simulate our systems at are shown in Figure 2.3. All the potentials are reported in units of k_bT.

The potentials used are coarse grain implicit solvent model. Atomistic potentials have a lot of detail in them (bonds, bends torsions for each atom) and it is expensive to carry out the simulations using atomistic potentials. Therefore coarse graining is done to save computational time. Coarse graining captures the thermodynamic properties and behavior of molecules in the system without the atomistic detail, making calculations more efficient. PEO PEO non-bonded interaction in the coarse grained implicit solvent model was obtained using the Inverted Boltzmann method. PEO is modeled as a bead spring model where each ethylene oxide unit is represented by a bead having a radius of

4A (24).

The behavior of the tube in water is known from atomistic simulations. The bare tubes will behave the same in all the systems simulated. Therefore as the behavior of this tube is known we represent the tube as a single line of force, we do not need to explicitly represent each carbon atom. This force/behavior of the tubes is obtained from atomistic simulations. The mass of the tube is carried by two atoms at the bottom and a atom is located in the center to track the position of the tube. Figure 2.4 represents how atomistic CNT is mapped onto the coarse grained simulations carried out. The two blue atoms at the bottom carry the mass of the tube. The red atom in the center is to track the position of the tube as it moves in the simulation. This coarse graining saves a lot of computational time and makes time scales which are not achievable by atomistic simulations accessible. The next chapter discusses the results from the simulations.

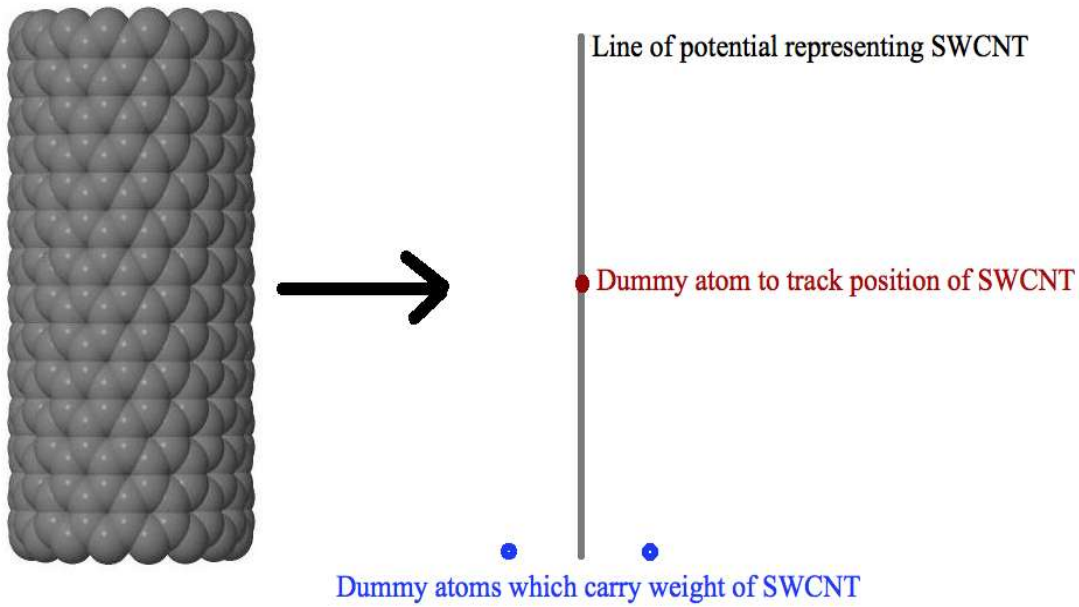

Figure 2.4: CNT mapping in coarse grained simulations

CHAPTER 3

RESULTS

The results below are divided into three sections. The first section discusses the structure of the polymer between the PEO tethered nanotubes. The structure varies with the grafting density and chain length of PEO. In the second section the thermodynamic properties of the system are reported. Thermodynamics properties that are calculated include potential of mean force and energetic and entropic contributions. As discussed before, the simulations are carried at four different potentials, and the effect that these potentials have on the behavior of the systems is discussed in the final third section.

3.1 Structure

Simulations of 13 systems are carried out, these systems vary in polymer chain length and grafting density. The grafting density on the tubes varies from short sparse chains (8PEO3 system) to long dense chains (32PEO24 system). The polymer brush profile varies as a function of distance from the grafting points on the tube. The free ends of the chains have more probability to explore the conformational space (25). Figure 3.1 shows the number density profile of the polymer as a function of distance from the center of the tubes for all the systems.

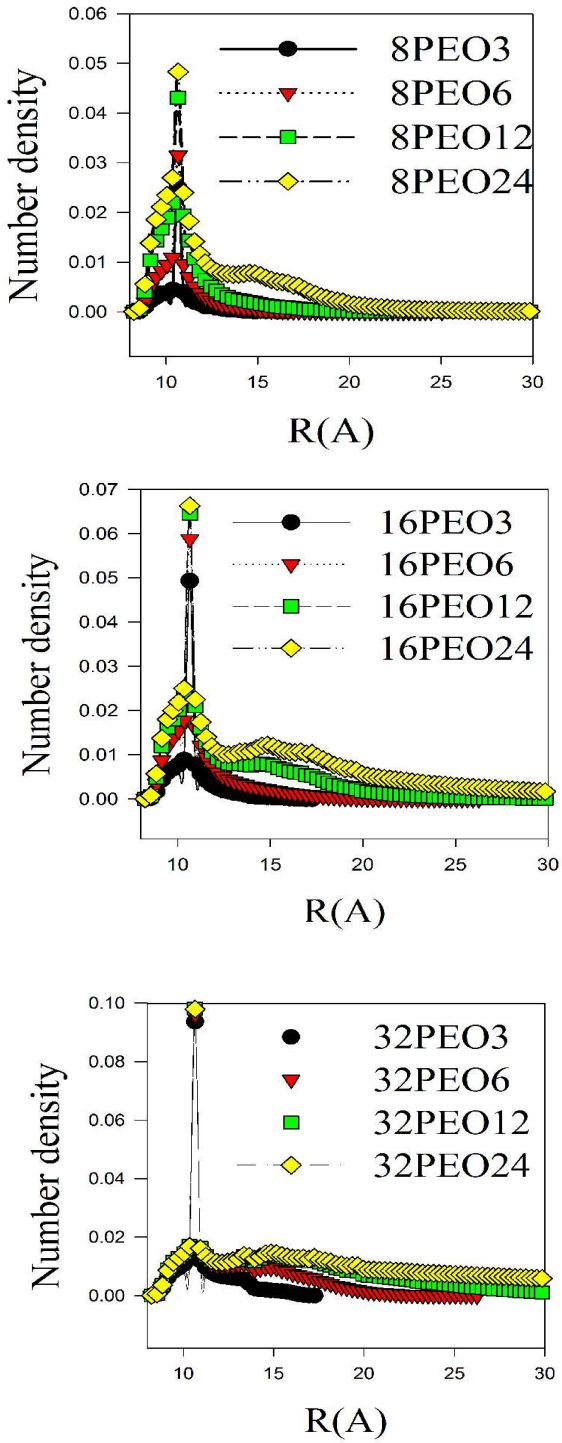

Figure 3.1: Number density profile of the PEO chains as a function of distance from the center of the tube.

The distance r = 0 in the figure corresponds to center of the tube. The number density shows how the PEO chains arrange themselves around the tube when the tubes are at a distance of furthest separation. That is equivalent to the single CNT structure. Figure 3.1 shows the number of PEO beads as we move from center of the tube to further out in the space, how the chains stretch themselves for the real system with full potentials (described in section 2.2). The graphs are plotted as a function of changing grafting density. The first graph shows the systems with 8 chains grafted on the surface. The different color plots in the graph are systems with changing chain length of PEO. The black color represents the shortest chain system of 3 monomers, the red for 6 PEO beads, green for medium chain length of 12 monomers and finally the yellow which is the longest chain of 24 monomers. The second and the third graph are for 16PEO beads and 32PEO beads grafting density respectively.

As we can see in each graph, for increasing chain length of the PEO the curve gets flatter. With increasing molecular weight, the curve gets flatter following a hyperbolic tangent shape. This effect is pronounced in the 32PEO24 system, which represents the highest grafting density and longest chain length system in the study. At lower grafting densities the polymer chains have more potential to explore the conformational space compared to a denser system.

The effect that increasing the chain length has on brush profile is similar to the effect that decreasing the radius of curvature of tubes has on the brush profiles of polymers (25). Up to a distance from the tube all chains are stretched equally and a specific number of polymer segments are present in this part of the brush, the rest are in the parabolic profile of the brush. From Figure 3.1 it can be seen that there is significant

difference in the shape of brush profiles as the grafting densities and the chain lengths are varied. The effect of varying the potentials (discussed in section 2.2) on structure of CNT is discussed in section 3.3.

3.2 Thermodynamic properties

Potential of mean force

The potential of mean force (PMF) is a way to express the free energy of a system as a function of a reaction coordinate. There are forces acting on each particle from all the other particles present in the system. These forces may try to move the particles apart or closer together depending on the type of their interaction. PMF is the force required to keep the particles separated at a particular given distance. In the simulations of a tube tethered with PEO, the reaction coordinate was equal to the distance between the center of the two tubes. The tubes are constrained at a fixed center of mass separations. Force is applied on the tubes to bring them closer together. This average force is integrated over the reaction coordinate using numerical methods to give the PMF. At each separation the simulation is run for 50 ns to allow sufficient time for the tethered polymers to attain most of the possible configurations. Free energy of the thirteen different systems as a function of distance between the center of two tubes for constant grafting density is shown in Figure 3.2 .

The PMF's are plotted as a function of constant grafting density (Figure 3.2) and constant molecular weight (Figure 3.3) of PEO chains.

a

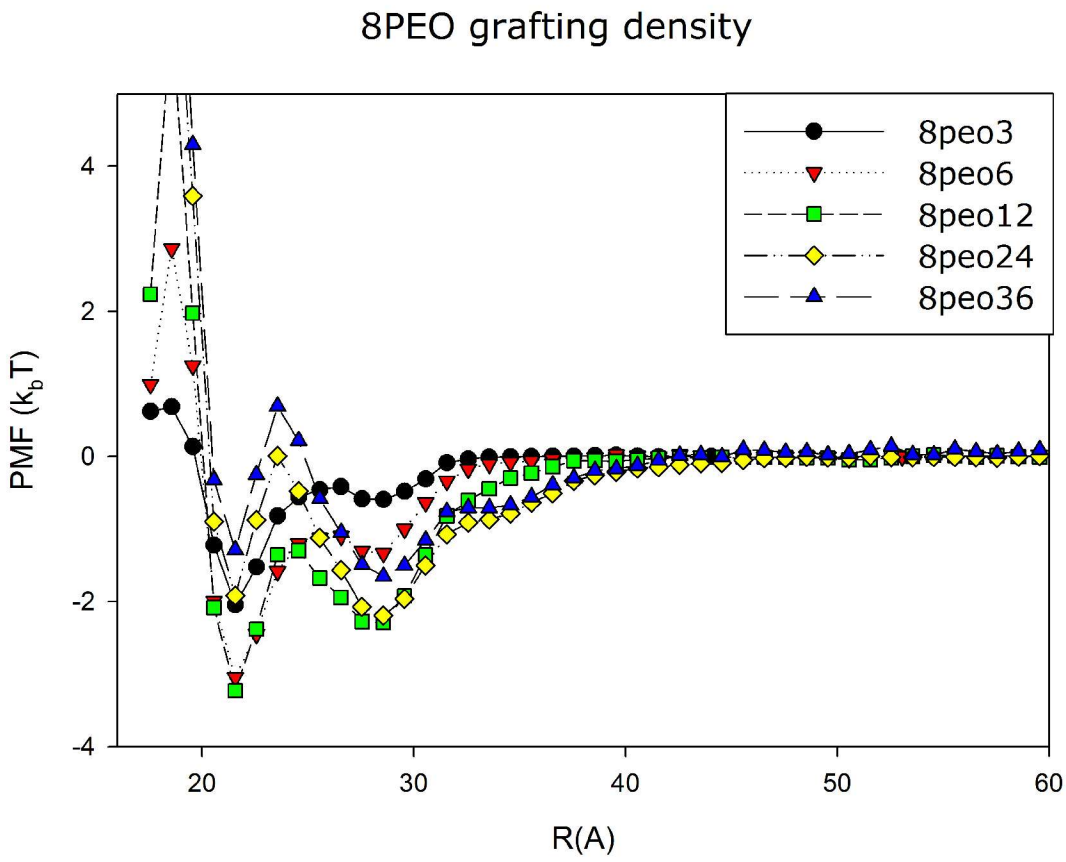

Figure 3.2 : Potential of mean force (PMF) as a function of separation (R), where R is the distance between center of two tubes as function of constant grafting density for (a) 8PEO system.

b

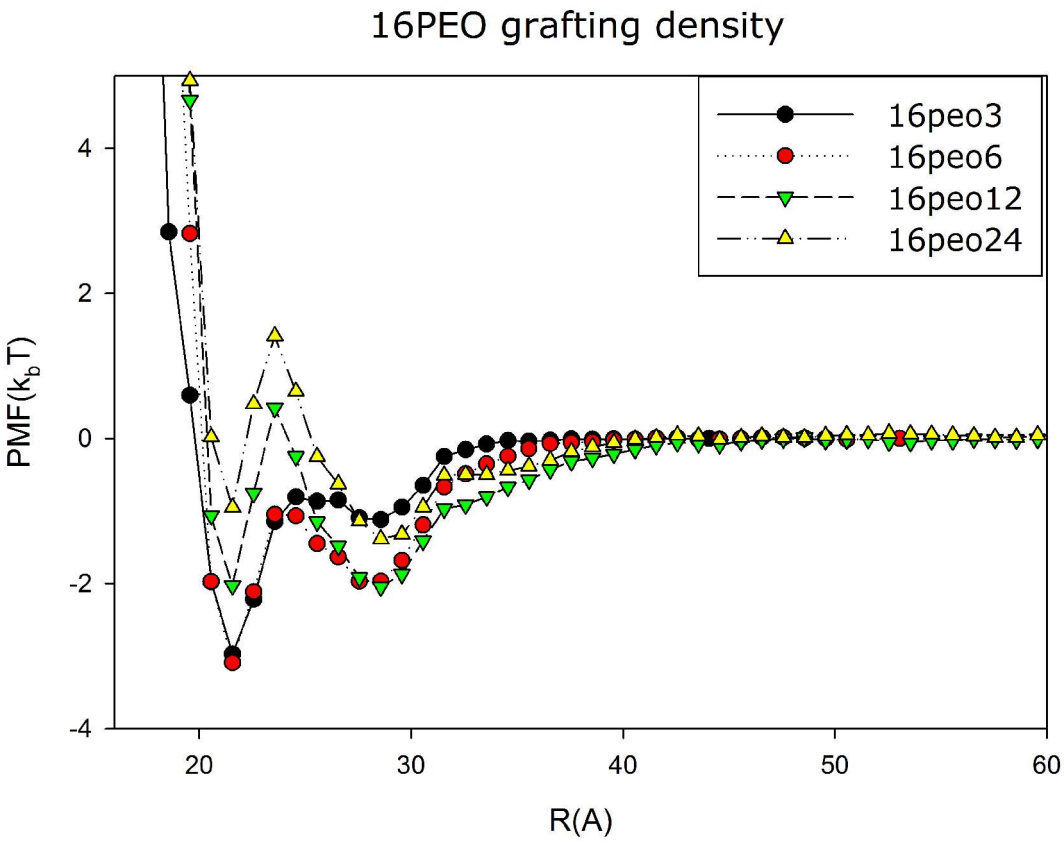

Figure 3.2: Cont. (b) 16PEO system.

c

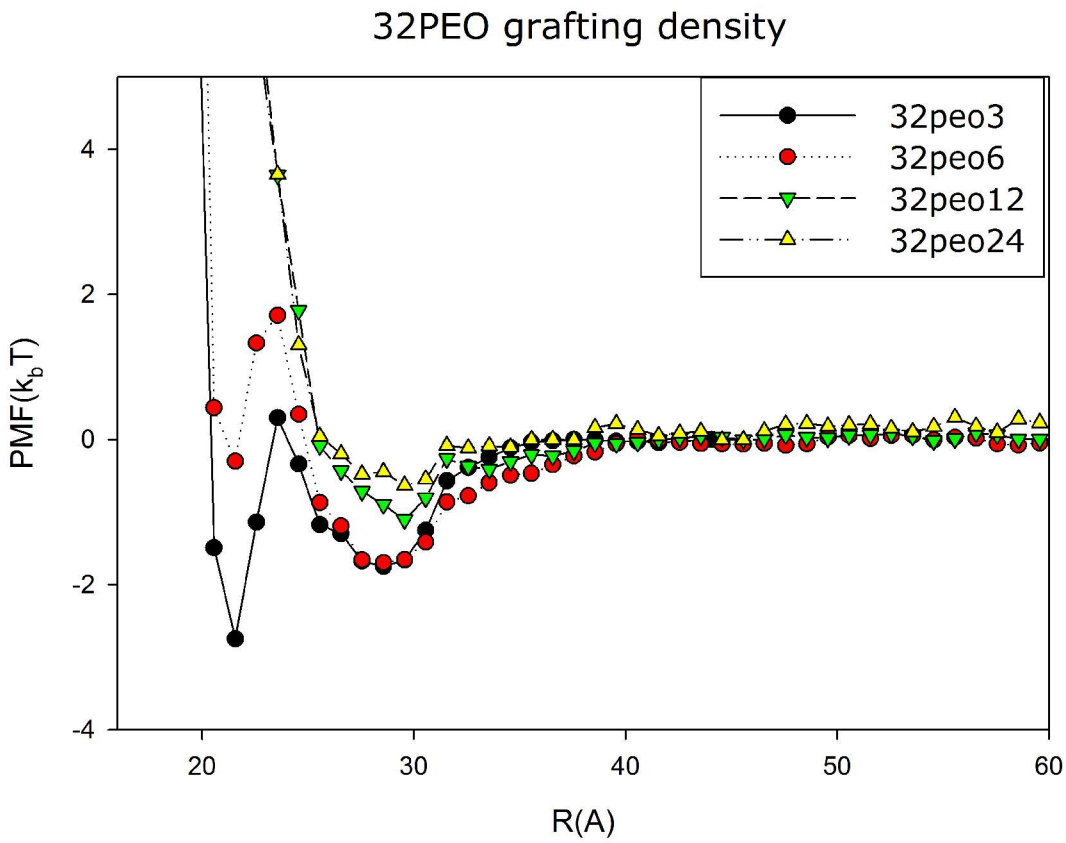

Figure 3.2: Cont. (c) 32PEO system.

a

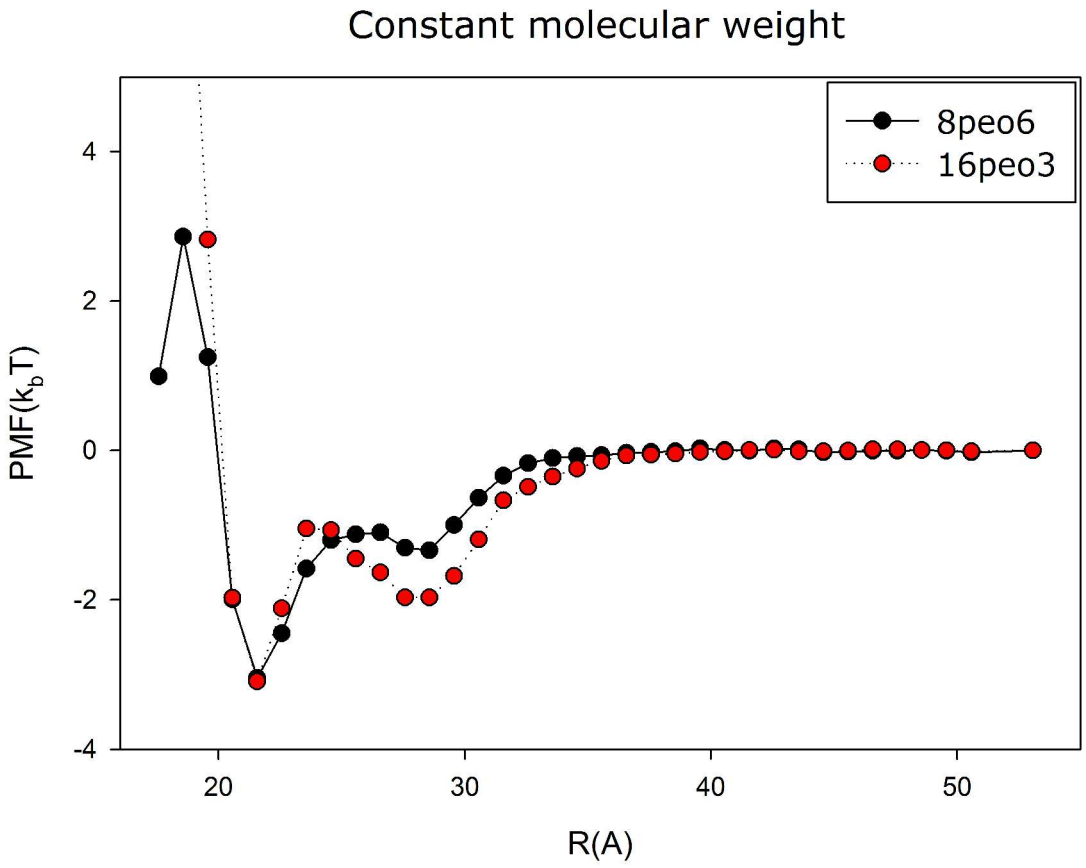

Figure 3.3: Potential of mean force (PMF) as a function of separation (R), where R is the distance between center of two tubes as function of constant molecular weight for (a) 0.032 PEO monomers per unit area of tube systems.

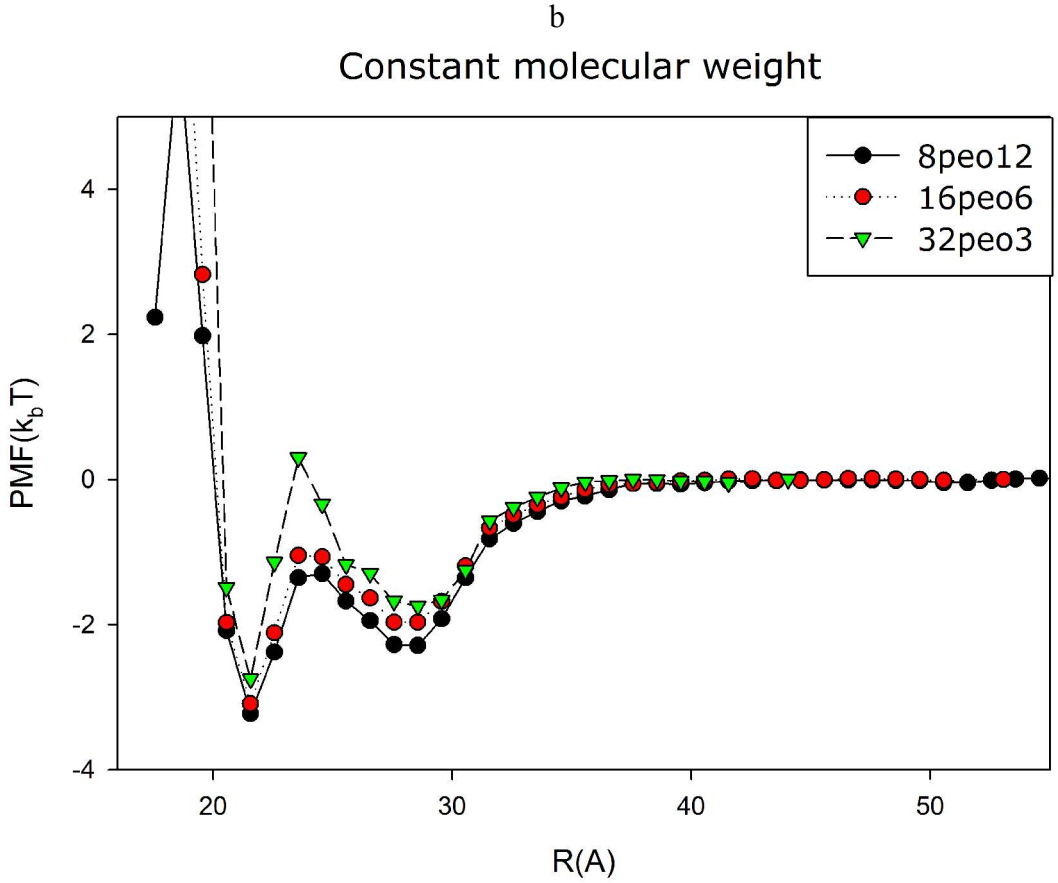

Figure 3.3: Cont. (b) 0.064 PEO monomers per unit area of tube systems.

c

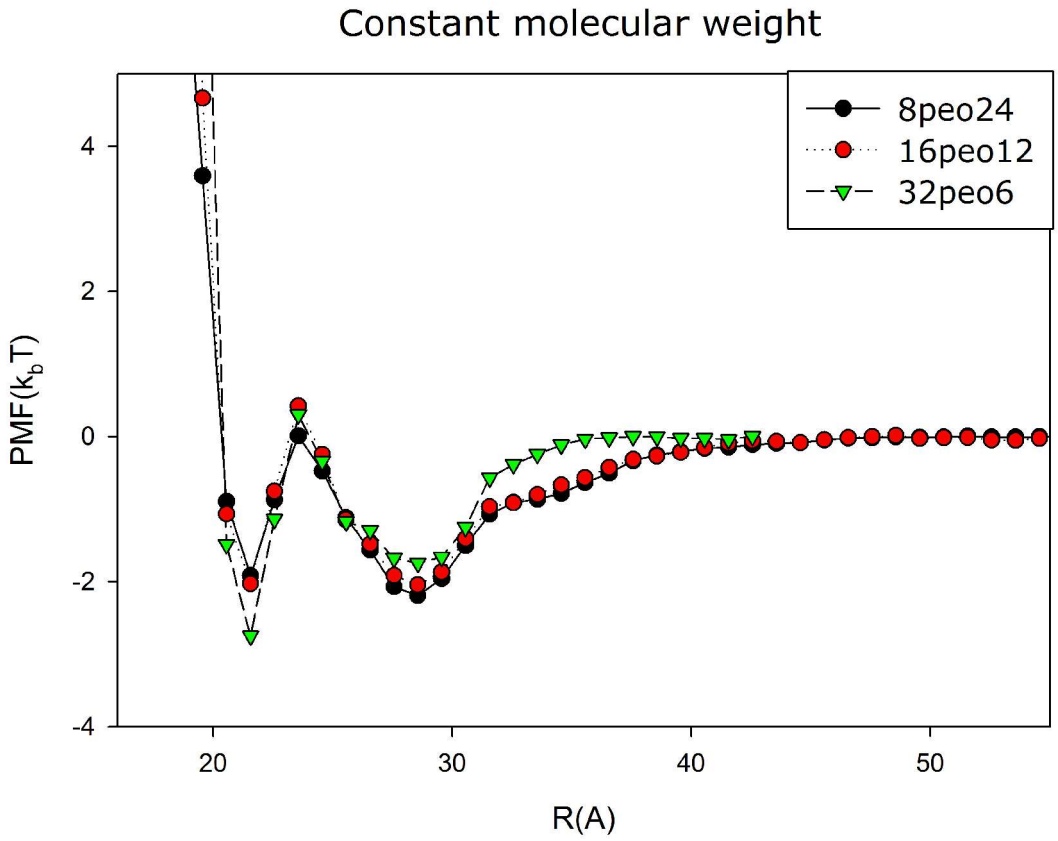

Figure 3.3: Cont. (c) 0.127 PEO monomers per unit area of tube systems.

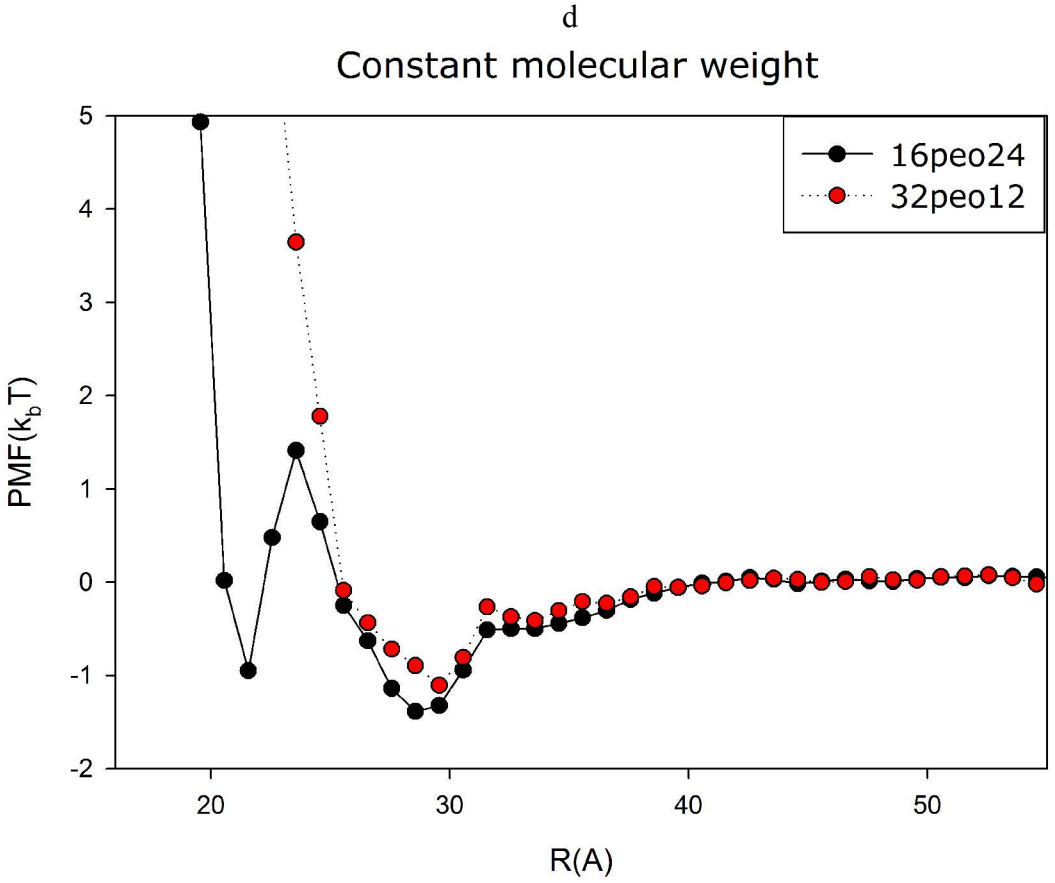

Figure 3.3: Cont. (d) 0.255 PEO monomers per unit area of tube systems.

The graphs are plotted as a function of constant grafting density (Figure 3.2) and constant molecular weight (Figure 3.3). All PMF's are reported in units of k_bT. The PMF's shown do not include the interaction between tube-tube. The tube-tube interaction remains the same irrespective of the changing molecular weight of the PEO chains. Also the minima that occurs in tube-tube interaction is at very distances of R=15.9A. This distance is not reached due to the repulsive barrier introduced by the PEO chains at R=20A. Therefore we can exclude the tube-tube interaction. Most of the systems have similar qualitative shape with two minimas and a huge repulsive barrier at very close distances. At large separations, for all the systems, there is no interaction between polymer grafted tubes, that is, the PEO chains on one tube are not influenced by the presence of PEO on the second tube. The free energy of the system at this point is independent of the separation distance, and the PMF is flat in this region.

However, at very close distances, where the huge repulsive barrier is seen (R= 20-21 A) more and more polymer is squeezed between the surface of tubes. All the surface sites are taken up at this close distance. Due to increasing steric repulsion it becomes unfavorable kinetically to add more polymer between the surfaces of the tubes even though it is favorable energetically. This gives rise to a huge repulsive barrier, beyond which the distance between the tubes cannot be decreased. There are two minimas present, the first minimum at R = 23 A is deeper than the second minimum at R = 29 A for most of the systems. The second minimum occurs when PEO chains from one tube starts feeling the presence of the chains attached to other tube. The PEO chains from one tube also start feeling the presence of the second tube as the tubes are brought closer together. The first minimum is due to the strong tube-PEO attraction. When the two tubes

approach each other, PEO chains from one tube try to reach the surface of the other tube.

At the second minima there are two 'layers' of PEO beads present and as we bring the tubes closer we squeeze out one layer, which gives rise to the smaller repulsive barrier . Then we have only one layer of PEO beads present at the first minima and by bringing the tubes closer together we are trying to remove that layer which gives rise to the higher repulsive barrier at very close distances.

At a constant grafting density (8PEO, 16PEO, 32PEO), shown in Figure 3.2(a), Figure 3.2(b) and Figure 3.2(c), the relative difference between the two minima's for smaller chain lengths is greater than the relative difference between two minimas of longer chain lengths. This indicates that longer chains give rise to many body effects, increasing the strength of entropic interaction. The strength of the repulsive barrier to reach the first minimum increases with increasing chain length at a given constant grafting density. This is expected, as increasing grafting density results in greater number of polymers present to take up the available surface sites. In some systems (8PEO24, 16PEO12, 16PEO24), due to presence of more steric effects, the depth of the minima is reduced and is almost comparable to the first minima. For higher molecular weight systems (32PEO12, 32PEO24), there is no first minima. The repulsive barrier after the second minima itself is so high that the system cannot overcome the entropic effects to reach the first minima. The steric effects are more pronounced for these systems as there is a larger amount of polymer resulting from higher grafting density compared to other systems. The 32PEO6 and 32PEO3 systems have a first minima as it has short chain chain unlike the other two systems with the same grafting density. The steric effect for 32PEO6 and 32PEO3 systems are less pronounced and hence the repulsive barrier can be

overcome by the tube-PEO energetic interaction.

For systems having the same molecular weight (Figure 3.3) the PMFs are different. Importantly, the difference in systems with constant molecular weight is more pronounced in systems with higher grafting density. Due to grafting density, PMF of 32PEO6 is different from 8PEO24 and 16PEO12 as shown in Figure 3.3(c). Also PMF of 32PEO12 system is different from 16PEO24 even though they have the same molecular weight as seen in Figure 3.3(d).

Ideally the PMF should be such that, there are slight attractions in the system which multi body effects can overcome but not so strong that the system will phase separate. As it can be seen in Figure 3.2 and Figure 3.3 both steric effects and the attractive interactions compete to give rise to minimas and repulsive barriers in the system. The shape of the PMF can be manipulated by changing the chain length and grafting density of the polymer.

Energy and entropic contributions to the PMF

Free energy of a system is given by

$$\Delta G = \Delta H - T\Delta S$$

The entropic contribution ($-T\Delta S$) is obtained as the difference between free energy (PMF) and energy (ΔH). Entropic effects arise mainly from the polymer's conformational degrees of freedom between the cylindrical surfaces. Presence of a surface reduces the number of allowed conformations and this loss in entropy gives rise to a repulsive

interaction between polymers and surface, especially at very close distances. The energy of the system (ΔH) can be decomposed into two components, one from tube-PEO and second from PEO-PEO. As discussed earlier, tube-PEO and PEO-PEO have favorable energetic interactions in water, and this creates an energetically favorable environment to have more polymer between the surface of tubes.

Attractive forces between tube-PEO compete with entropic forces to determine the final structure. Figure 3.4 shows the PMF, PEO-PEO energy, tube-PEO energy, total energy and entropic interaction of three systems. The 8PEO3 system is the lowest grafting density, shortest chain length system (Figure 3.4(a)); 16PEO12 is medium grafting density and medium chain length system (Figure 3.4(b)); 32PEO24 is the largest grafting density, longest chain length system (Figure 3.4(c)). It can be seen that PEO-PEO interaction is favorable energetically in water for all systems but is much weaker than tube-PEO interaction in water. Only for the 32PEO24 system is the PEO-PEO energy greater than tube-PEO energy. The total energy of the system (yellow curve) has the same qualitative shape as that of contribution of tube-PEO interaction energy (red curve). 32PEO12 and 32PEO24 systems are entropy driven at closer distances. Also, with increasing chain length, the entropic contribution increases for a given graft density. This is expected, as longer chain lengths give rise to many body effects.

We can conclude that PEO-PEO energy doesn't really affect the phase behavior of the system and it is the tube-PEO and the entropic contribution at closer distance that determine the phase behavior.

a

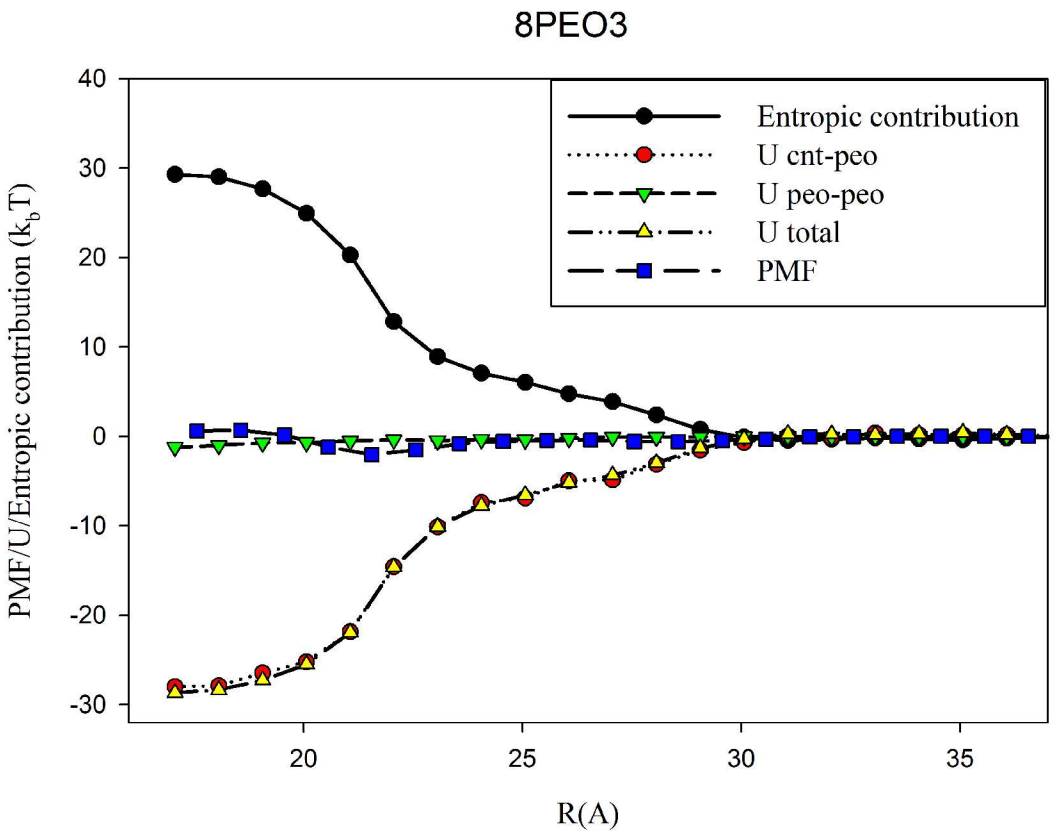

Figure 3.4: PMF, CNT-PEO energy, PEO-PEO energy, total energy and entropic contribution as a function of separation between center of two tubes for (a) 8PEO3 system.

b

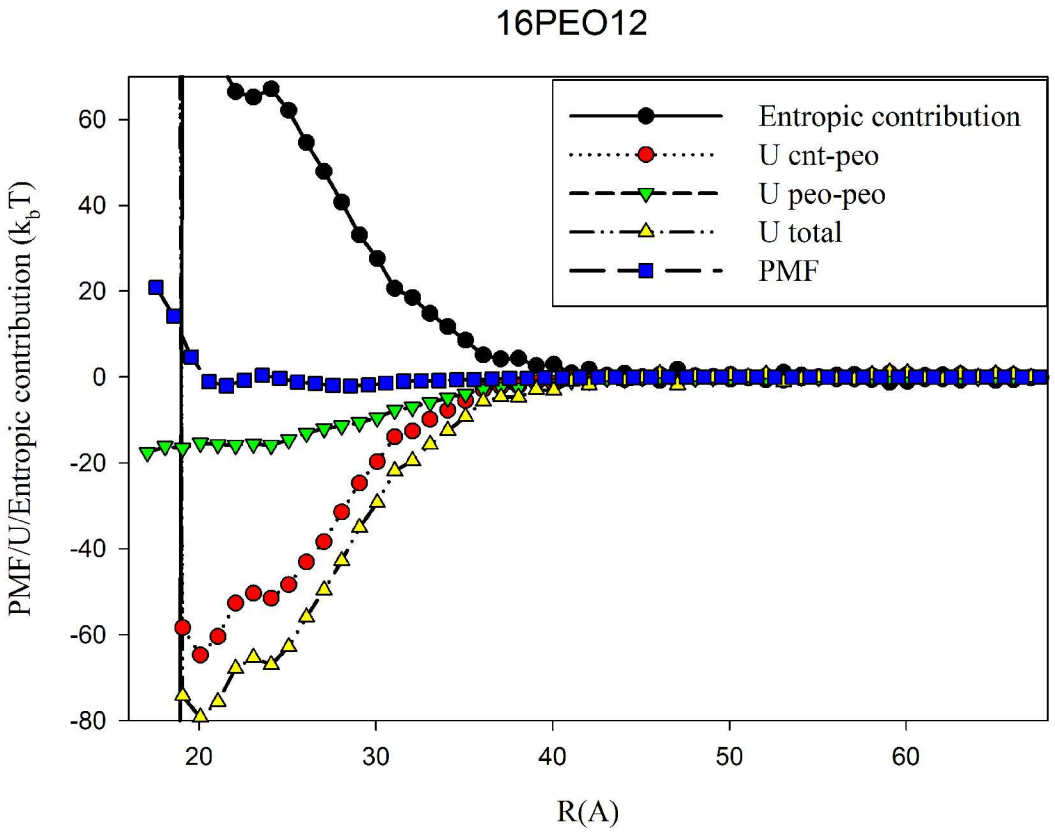

Figure 3.4: Cont. (b) 16PEO12 system.

c

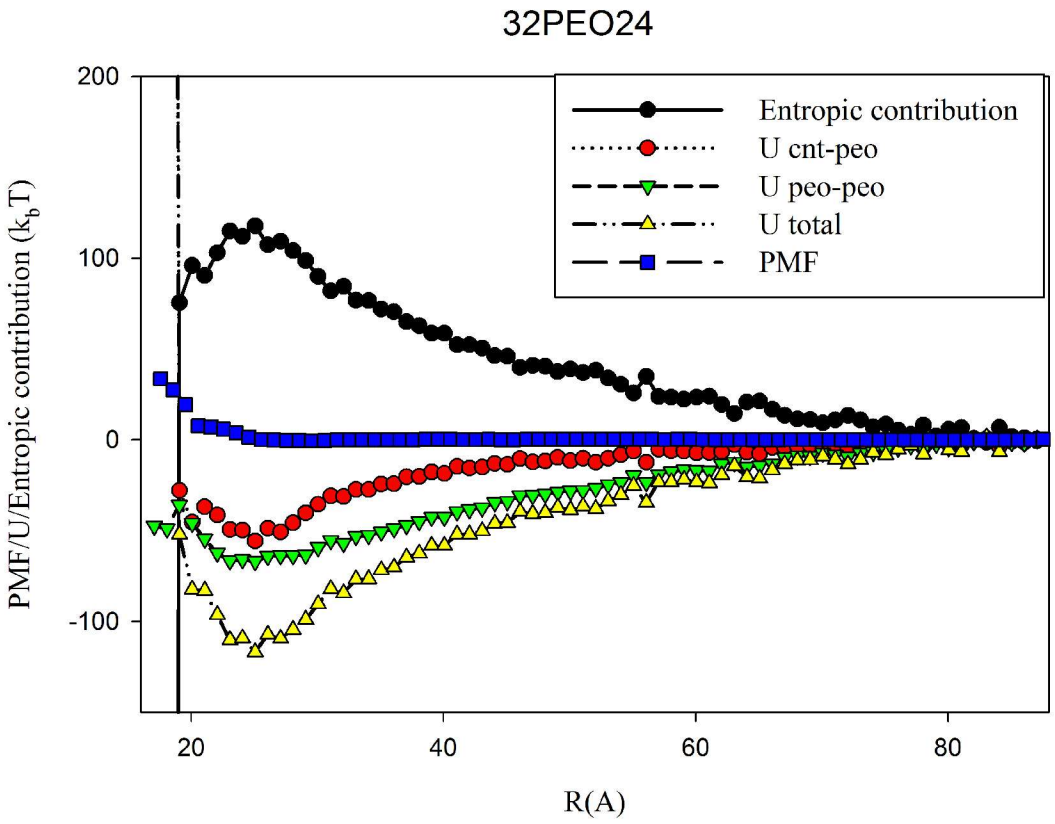

Figure 3.4: Cont. (c) 32PEO24 system.

3.3 Influence of intermolecular potential

All the 13 systems shown in Table 2.1 are simulated at four different potentials as described in section 2.2. By making each interaction in the system repulsive at a time we can understand the relative importance of that particular interaction. For example, in the Repulsive CNT-PEO potential, the interaction between tube and PEO is repulsive, therefore the only potential that has an effect on the system is between PEO-PEO and this way we can better understand the role of PEO-PEO interaction.

First we discuss how the intermolecular potentials affect the structure of a single CNT and how that affects the brush heights of the polymer. The brush height is calculated as:

$$H = \frac{(3\int_0^\infty \rho(r) r^{(2)} dr)}{(2\int_0^\infty \rho(r) r\, dr)}$$

where H is the brush height in A, ρ is the number density and r is the distance from the center of the tube. The number density was calculated and reported for all the systems in section 3.1. The brush heights for all the systems at four different potentials are reported in Table 3.3. The brush heights are in units of Angstroms.

Table 3.3: Brush height (A) of PEO chain for all systems for four different intermolecular potentials.

Brush height	8peo3	8peo6	8peo12	8peo24
Real	16.27	16.54	17.26	20.77
Repulsive All	17.86	20.71	27.13	37.05
Repulsive CNT PEO	17.58	20.62	26.59	35.4
Repulsive PEO PEO	16.28	16.61	17.76	23.46
Brush height	16peo3	16peo6	16peo12	16peo24
Real	16.34	17.47	20.8	28.44
Repulsive All	17.94	21.51	28.86	40.83
Repulsive CNT PEO	17.88	17.92	22.39	33.01
Repulsive PEO PEO	16.39	17.92		38.44
Brush height	32peo3	32peo6	32peo12	32peo24
Real	16.99	20.26	26.09	38.1
Repulsive All	18.52	23.17	31.54	45.98
Repulsive CNT PEO	18.27	21.25	28.63	42.88
Repulsive PEO PEO	17.32	22.53	29.96	42.55

For the Repulsive All systems where all the interactions (tube-PEO, PEO-PEO) are repulsive, the chains are stretched out more, therefore having a greater brush height as compared to other potentials. The brush heights of Repulsive PEO-PEO potential are close to Real system implying that PEO-PEO potential is not so important in deciding the structure of the polymer. Also for a given potential and grafting density, the brush heights increase with increasing chain lengths as expected.

The coordination number for all systems simulated at four different potentials is calculated. The coordination shell is defined as the number of monomers present between 8 A<R<13 A, where R here is the distance from the center of tubes. The coordination number is defined from the radial distribution function of polymers around the tube. Radial distribution function gives us the probability of finding an atom at a distance from a given atom. The width of the first peak is defined as the coordination shell. Coordination number is the number of atoms surrounding an atom *i* in a sphere of a radius *r*. Two types of monomers are defined in the coordination shell: those that belong to the grafted tube and those that originate from the second tube .

Figure 3.5 shows the number of monomers present in the coordination shell that come from the other tube for the 16PEO12 system for all the four potentials as function of separation between the two tubes. At far distances when the tubes are sufficiently separated, there are no monomers in the coordination shell, thats is why the coordination number is almost flat at zero. As the tubes are brought closer together, more and more monomers from the other tube are added to the coordination shell. When there is no energy in the system (Repulsive_All) only entropic interactions are present and there are considerably fewer number of monomers in the coordination shell as compared to real potential.

Figure 3.6 shows the coordination number of monomers from other tube for the 32PEO24 system which is the highest grafting density and longest chain length system as function of separation between two tubes. At higher grafting densities (32PEO system), as shown in Figure 3.6, the difference between different potentials (as seen in 16PEO system, Figure 3.5) reduces.

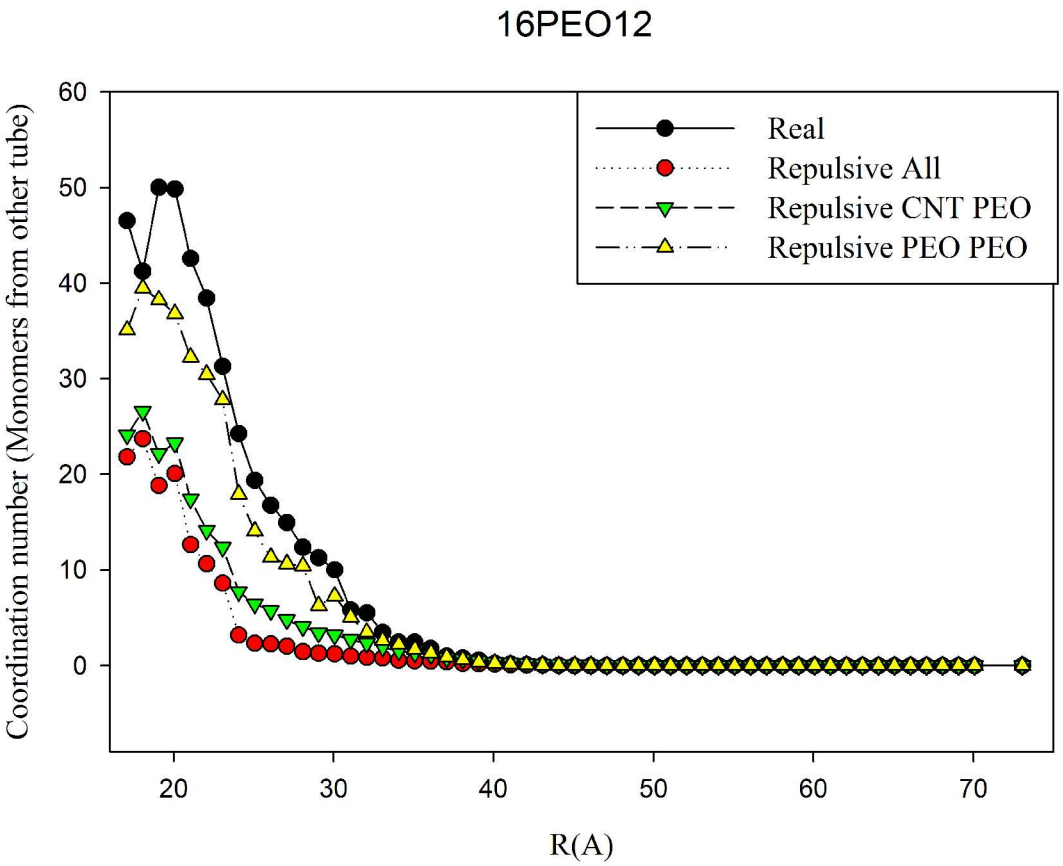

Figure 3.5: Coordination number (Number of monomers that come from other tube) for 16PEO12 system as function of separation between two tubes.

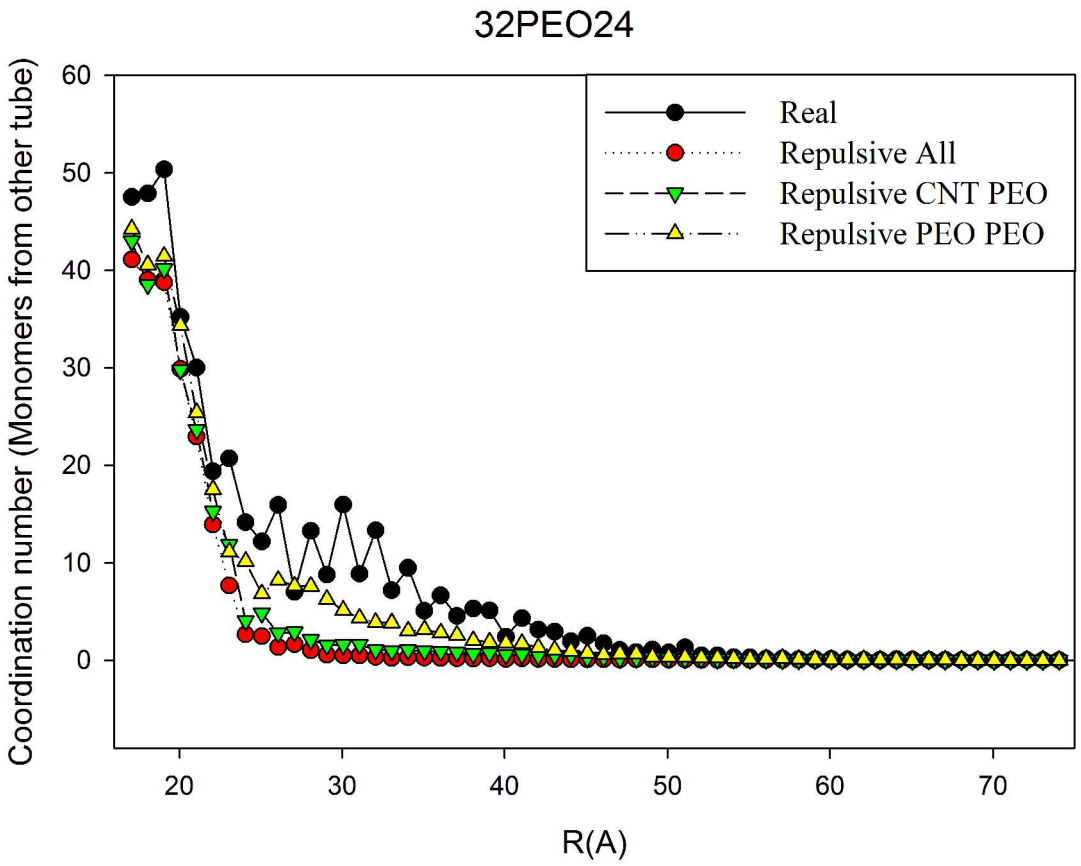

Figure 3.6: Coordination number (Number of monomers that come from other tube) for 32PEO24 system as a function of separation between two tubes.

In simulations of Repulsive_All potentials, no tendency of aggregation is seen, as all the potentials are set to be repulsive. Systems simulated with Repulsive_PEO PEO show the same qualitative behavior as systems with Real potential, indicating that there are no effects resulting from chains being plastered on surface. Number of monomers in the coordination shell for Repulsive PEO-PEO potential is almost similar to that of real system, indicating that the interaction between tube and polymers is most important. For higher grafting densities energy between CNT PEO or PEO PEO hardly plays a role in number of monomers present in coordination shell.

Figure 3.7 shows the PMF for all the potentials for 16PEO12 system. Repulsive PEO PEO has same qualitative behavior as Real potentials. Repulsive All system is similar to Repulsive CNT PEO. All the other systems show behavior similar to that illustrated in Figure 3.7. There is no effect of chain wrapping that is seen in any of the systems.

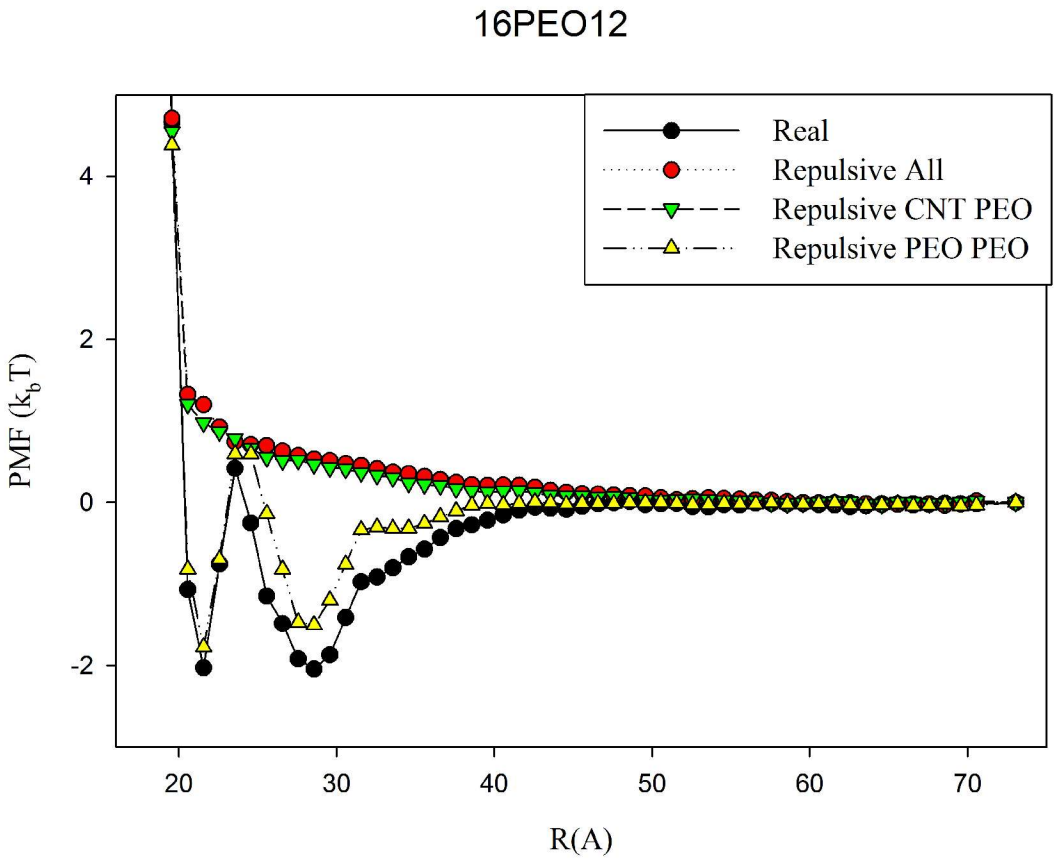

Figure 3.7: PMF of 16PEO12 system for all the four potentials as a function of separation between two tubes.

CONCLUSIONS

This work shows that tethering polymer to the surface of nanotubes gives rise to several interactions between tube-PEO, PEO-PEO and steric crowding between the tubes that would allow controlled self-assembly behavior. Previous simulation studies have studied polymer grafted tubes but showed presence of a purely repulsive interaction due to the steric crowding caused by presence of polymer where the strength and range of repulsions are monotonic increasing functions of both chain length and polymer surface coverage. The simulations carried out show presence of more complex interactions which guide the behavior of self-assembly. The interaction between tube-PEO is the strongest interaction in the system. This favorable interaction coupled with the entropic effects gives rise to two minimas in the free energy of the system. The strength and range of the minimas can be manipulated by changing the grafting density and chain length of the tethered PEO. Higher grafting densities with longer chain lengths PEO systems have only one minima as entropic effects dominate at close distances of the tube.

In the simulations infinitely long rods are used, further work would focus on how energy/properties scale with length in rods. We would also like to investigate if virial coefficient is a sufficient measure to conclusively predict if the tubes would phase separate or self-assemble. Further extension would be to investigate multiple tube geometries and their phase behavior.

REFERENCES

(1) Liu, P. *European Polymer Journal* **2005**, *41*, 2693-2703.

(2) Salvetat, J.P. *AIP Conference Proceedings* **1998,** *442,* 467-80.

(3) White, C. T. *Physical review. B, Condensed Matter* **1993**, *47.9*, 5482-8.

(4) Vairavapandian, D.; Vichchulada, P.; Lay, M. D. *Analytica Chimica Acta* **2008**, *626*, 119-29.

(5) Saito, Y. *MHS'99. Proceedings of 1999 International Symposium on Micromechatronics and Human Science (Cat. No.99TH8478)* **1999**, 43-49.

(6) Paradise, M.; Goswami, T. *Materials & Design* **2007**, *28*, 1477-1489.

(7) Ruoff, R. *Carbon* **1995**, *33*, 925-930.

(8) Endo, M.; Hayashi, T.; Kim, Y. A.; Muramatsu, H. *Japanese Journal of Applied Physics* **2006**, *45*, 4883-4892.

(9) Ajayan, P. M.; Zhou, O. Z. *Carbon Nanotubes Synthesis, Structure, Properties and Applications*, Springer Publications **2001**, pp 391-425.

(10) Thess, a; Lee, R.; Nikolaev, P.; Dai, H.; Petit, P.; Robert, J.; Xu, C.; Lee, Y.; Kim, S.; Rinzler, A.; Colbert, D.; Scuseria, G.; Tomanek, D.; Fischer, J.; Smalley, R. *Science (New York, N.Y.)* **1996**, *273*, 483-7.

(11) Li, L.; Bedrov, D.; Smith, G. D. *The Journal of Physical Chemistry. B* **2006**, *110*, 10509-13.

(12) Alexandridis, P. *Current Opinion in Colloid & Interface Science* **1996**, *1*, 490-501.

(13) Pasut, G.; Veronese, F. *Progress in Polymer Science* **2007**, *32*, 933-961.

(14) Zalipsky, S. *ACS Symposium Series* **1997**, *680,* 1-13.

(15) Bedrov, D.; Smith, G. D.; Li, L. *Langmuir: The ACS Journal of Surfaces and Colloids* **2005**, *21*, 5251-5.

(16) Shvartzman-cohen, R.; Nativ-roth, E.; Baskaran, E.; Levi-kalisman, Y.; Szleifer, I.;Yerushalmi-rozen, R.; Lafayette, W.; Ilse, T.; Science, N. *Macromolecules* **2004**, *126* 14850-14857.

(17) Nativ-roth, E.; Shvartzman-cohen, R.; Florent, M.; Zhang, D.; Szleifer, I.; Yerushalmi-rozen, R.; Sheva, B. *Nanotechnology* **2007**, *40*, 3676-3685.

(18) Zheng, X.; Xu, Q. *Technology* **2010**, *114*, 9435-9444.

(19) Yang, M.; Koutsos, V.; Zaiser, M. *The Journal of Physical Chemistry. B* **2005**, *109*, 10009-14.

(20) Sinsawat, A.; Anderson, K. L.; Vaia, R. A.; Farmer, B. L. *Polymer* **2003**, *41*, 3272-3284.

(21) http://www.eng.utah.edu/~gdsmith/lucretius.html (accessed March 10, 2011).

(22) Allen, M.; Tildesly D. *Computer simulations of liquids;* Oxford, **1989**, pp 6-9.

(23) Weeks, J. D. *The Journal of Chemical Physics* **1971**, *54*, 5237.

(24) Bedrov, D.; Ayyagari, C.; Smith, G. D. *Quantum* **2006**, *2*, 598-606.

(25) Wijmans, C. M.; Zhulina, E. B. *Macromolecules* **1993**, *26*, 7214-7224.